

# $\rho$ - $\omega$ mixing effects in relativistic heavy-ion collisions

Wojciech Broniowski and Wojciech Florkowski

*H. Niewodniczański Institute of Nuclear Physics, PL-31342 Kraków, Poland*

---

## Abstract

We show that even moderate excess of neutrons over protons in nuclear matter, such as in  $^{208}\text{Pb}$ , can lead to large  $\rho$ - $\omega$  mixing at densities of the order of twice the nuclear saturation density and higher. The typical mixing angle is of the order of  $10^\circ$ . The mixing may result in noticeable shifts of the positions and widths of resonances. We also analyze temperature effects and find that temperatures up to 50 MeV have practically no effect on the mixing.

---

Over the past few years considerable theoretical efforts have been made to understand in-medium properties of mesons [1,2]. Moreover, the measurement of dilepton spectra in CERES [3] and HELIOS [4] experiments at CERN provides a possibility of verifying various theoretical predictions concerning light vector mesons [5,6]. A number of medium effects is expected to occur in the  $\rho$  and  $\omega$  channels: shift of position of resonances, broadening of their widths, reduction of strength, emergence of collective branches, or mixing of states which have different quantum numbers in the vacuum.

The mechanism of mixing induced by the medium has a different origin than the mixing due to explicit symmetry-breaking terms in the Hamiltonian. It results from the breaking of the symmetry by the *medium*. A well-known example is the mixing of the scalar-isoscalar  $\sigma$  meson with the longitudinal component of the vector  $\omega$  meson [7]. It is allowed, since the matter state breaks the Lorentz invariance. Recently Dutt-Mazumder, Dutta-Roy and Kundu [8] analyzed the effects of isospin asymmetry in matter on  $\rho$ - $\omega$  mixing. Their analysis, carried out in the Walecka model [9], implies that at asymmetries such as in  $^{208}\text{Pb}$  and at nuclear saturation density the  $\rho$  and  $\omega$  mix with an angle of about  $2^\circ$ . In this Letter we show that the matter-induced  $\rho$ - $\omega$  mixing effects may in fact be much larger. Denote the correlator for vanishing 3-momentum  $\mathbf{q}$  in the coupled neutral  $\rho$  and

---

\* Research supported by the Polish State Committee for Scientific Research 2P03B-080-12

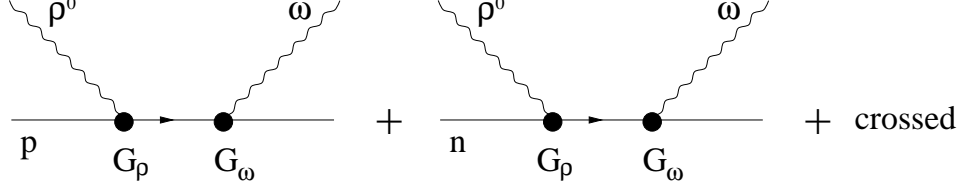


Fig. 1. Matter-induced mechanism of  $\rho$ - $\omega$  mixing.

$\omega$  channels by

$$\Pi^{\alpha\beta}(\nu, \mathbf{q} = 0) = \begin{pmatrix} \Pi_{\rho}^{\alpha\beta}(\nu) & \Pi_{\rho\omega}^{\alpha\beta}(\nu) \\ \Pi_{\rho\omega}^{\alpha\beta}(\nu) & \Pi_{\omega}^{\alpha\beta}(\nu) \end{pmatrix}, \quad (1)$$

where  $\nu$  is the energy variable. Our approach differs from that of Ref. [8]. Instead of using a particular model to describe the diagonal parts of (1), we choose a simple form which can mimic the results of various specific calculations:  $\Pi_v^{\alpha\beta}(\nu) = Z_v^{*-1} ((\nu - i\Gamma_v^*/2)^2 - m_v^{*2}) T^{\alpha\beta}$  where  $v = \rho, \omega$ . The asterisk denotes the in-medium values of the resonance position,  $m_v$ , width,  $\Gamma_v$ , and the wave-function renormalization,  $Z_v$ . The tensor  $T^{\alpha\beta} = \text{diag}(0, 1, 1, 1)$  enters for  $\mathbf{q} = 0$  [7,10,11]. Our parameterization incorporates basic features of mesons propagating in nuclear medium, such as the shift of the resonance position, broadening, and wave-function renormalization. We find this simple parameterization better for our purpose of analyzing the nature of  $\rho$ - $\omega$  mixing. Various specific calculations have substantially different predictions for  $\Pi_{\rho}^{\alpha\beta}$  and  $\Pi_{\omega}^{\alpha\beta}$ , depending on physics involved [10–27].

For the off-diagonal term of the correlator,  $\Pi_{\rho\omega}^{\alpha\beta}$ , responsible for the mixing in asymmetric matter, we choose the same mechanism as in Ref. [8], namely the interaction of vector mesons with the Fermi sea of protons and neutrons. This is depicted in Fig. 1. The coupling of  $\omega$  to the proton and neutron is equal with the same sign, and the coupling of  $\rho^0$  to the proton and neutron is equal and *opposite*. As a result, the sum of diagrams in Fig. 1 does not vanish if we have isospin-asymmetric matter, *i.e.* excess of neutrons over protons. The coupling of vector mesons to nucleons is described by the Lagrangian

$$L_{\text{int}} = \bar{\psi} (\tau^a G_{\rho,\alpha} \rho_a^\alpha) \psi + \bar{\psi} (G_{\omega,\alpha} \omega^\alpha) \psi, \quad G_{v,\alpha} = g_v \left( \gamma_\alpha - \frac{\kappa_v}{2M} \sigma_{\alpha\beta} \partial^\beta \right), \quad (2)$$

where  $\psi$ ,  $\rho_a^\alpha$  and  $\omega^\alpha$  are the nucleon,  $\rho$  and  $\omega$  fields, and  $M$  denotes the nucleon mass in the vacuum. Note that we include the tensor coupling of mesons, which is quantitatively important. Following Ref. [18] we use two parameter sets:

$$\begin{aligned} \text{I:} & \quad g_\rho = 2.63, \quad \kappa_\rho = 6.0, \quad g_\omega = 10.1, \quad \kappa_\omega = 0.12, \\ \text{II:} & \quad g_\rho = 2.72, \quad \kappa_\rho = 3.7, \quad g_\omega = 10.1, \quad \kappa_\omega = 0.12. \end{aligned}$$

This parameterization follows from the vector meson dominance model [28]. The basic difference between the two sets is the value of  $\kappa_\rho$  [29].

Applying the usual formalism [7,18] one finds that the off-diagonal matrix element in Eq. (1), describing the mixing of  $\rho^0$  and  $\omega$  (at  $\mathbf{q} = 0$ ) is given by

$$\begin{aligned} \Pi_{\rho\omega}^{\alpha\beta}(\nu, \mathbf{q} = 0) = & -i \int \frac{d^4k}{(2\pi)^4} \left\{ \text{Tr}[G_\rho^\alpha(\nu)S_D^p(k^0 + \nu, \mathbf{k})G_\omega^\beta(-\nu)S_F^p(k)] - \right. \\ & \left. \text{Tr}[G_\rho^\alpha(\nu)S_D^n(k^0 + \nu, \mathbf{k})G_\omega^\beta(-\nu)S_F^n(k)] \right\} + (F \leftrightarrow D) \equiv T^{\alpha\beta}\Pi_{\rho\omega}(\nu), \end{aligned} \quad (3)$$

where  $S_D^{p,n}(k)$  and  $S_F^{p,n}(k)$  denote the density part and the free part of the Dirac propagator for the proton and neutron [7]. Expression (3) incorporates the Fermi sea effects and the Pauli blocking. Explicit evaluation gives

$$\begin{aligned} \Pi_{\rho\omega}(\nu) = & \frac{2}{3}g_\rho g_\omega \int \frac{d^3k}{(2\pi)^3 E^*(k)} \frac{\theta(k_n - |\mathbf{k}|) - \theta(k_p - |\mathbf{k}|)}{\nu^2 - 4E^*(k)^2} \times \\ & \left[ 8E^*(k)^2 + 4M^*(k)^2 + 3(\kappa_\rho + \kappa_\omega) \frac{M^*}{M} \nu^2 + \kappa_\rho \kappa_\omega \frac{E^*(k)^2 + 2M^{*2}}{M^2} \nu^2 \right], \end{aligned} \quad (4)$$

where  $k_p$  and  $k_n$  are the proton and neutron Fermi momenta,  $M^*$  is the nucleon scalar self-energy in medium, and  $E^*(k) = \sqrt{M^{*2} + k^2}$ . As already mentioned, in symmetric matter, where  $k_p = k_n$ , the proton and neutron contribution to Eqs. (3,4) cancel and  $\Pi_{\rho\omega}(\nu)$  vanishes. In asymmetric matter  $k_n > k_p$ , and we get a net contribution to  $\Pi_{\rho\omega}(\nu)$ .

The proton and neutron densities are equal to  $\rho_{p,n} = k_{p,n}^3/(3\pi^2)$ , and the baryon density  $\rho_B$  and the isospin asymmetry  $x$  are equal to  $\rho_B = \rho_p + \rho_n$  and  $x = (\rho_n - \rho_p)/\rho_B$ . At low  $x$  it can be easily shown that  $\Pi_{\rho\omega}(\nu)$  is linear in  $x$ . It remains linear for asymmetries accessible in heavy-ion collisions. If in addition we expand Eq. (4) at small  $\rho_B$ , we notice that  $\Pi_{\rho\omega}(\nu) \sim x\rho_B = \rho_n - \rho_p$ , in agreement with the low-density theorem for the scattering amplitude [30,31].

Finding the eigenvalues of the matrix (1) is equivalent to solving the following equation:

$$\text{Det} \begin{pmatrix} (\nu - i\Gamma_\rho^*/2)^2 - m_\rho^{*2} & \sqrt{Z_\rho^* Z_\omega^*} \Pi_{\rho\omega}(\nu) \\ \sqrt{Z_\rho^* Z_\omega^*} \Pi_{\rho\omega}(\nu) & (\nu - i\Gamma_\omega^*/2)^2 - m_\omega^{*2} \end{pmatrix} = 0, \quad (5)$$

where we have moved the wave-function renormalization factors to off-diagonal terms in order to visualize that the results depend on the product  $Z_\rho^* Z_\omega^*$ . Equation (5) yields eigenvalues  $\nu_1$  and  $\nu_2$ , and the corresponding eigenstates  $|1\rangle$  and  $|2\rangle$ . Our convention is that in the absence of mixing, *i.e.* for  $x = 0$ , we have  $|1\rangle = |\rho\rangle$  and  $|2\rangle = |\omega\rangle$ . A commonly used measure of mixing of states is the mixing angle. Since the problem (5) is not hermitian, the eigenstates  $|1\rangle$  and  $|2\rangle$  are not orthogonal and we cannot define a single mixing angle. We find it useful to introduce two mixing angles,  $\theta_1$  and  $\theta_2$ , through the relations

$$|1\rangle = \cos \theta_1 |\rho\rangle + \sin \theta_1 |\omega\rangle, \quad |2\rangle = -\sin \theta_2 |\rho\rangle + \cos \theta_2 |\omega\rangle. \quad (6)$$

Since the matrix in (5) is complex, the mixing angle are in general complex.

Our results are shown in Table I, which contains 14 widely different cases. The table should be read from top to bottom. The first row labels the case. The second row gives the baryon density,  $\rho_B$ , in units of the nuclear saturation density  $\rho_0 = 0.17\text{fm}^{-3}$ . Five subsequent rows contain our choice of  $M^*$ ,  $m_\rho^*$ ,  $m_\omega^*$ ,  $\Gamma_\rho^*$ ,  $\Gamma_\omega^*$  and  $\sqrt{Z_\rho^* Z_\omega^*}$  for symmetric matter of density  $\rho_B$ . As already mentioned, the values for these quantities do not follow from any specific calculation, but are chosen according to experience accumulated by various existing calculations in the literature [10–27]. Most of our cases take  $\rho_B = 2\rho_0$ . We assume that at this density the nucleon mass drops to 50% of its vacuum value. The values of  $m_\rho^*$  and  $m_\omega^*$  are assumed to be between 450MeV and 650MeV. The widths take very different values. The wave function renormalization factors are assumed to be  $\sqrt{Z_\rho^* Z_\omega^*} = 0.7$ , or lower. Model calculations show that these factors get reduced rather significantly in nuclear medium. It is assumed that the coupling constants  $g_v$  and  $\kappa_v$  do not depend on density. The seven bottom rows of the table contain our results for the mixing at asymmetry  $x$  such as in  $^{208}\text{Pb}$ , *i.e.*  $x = x_{Pb} \equiv 44/208$ , and for parameter sets I and II. The quantities  $\nu_1$  and  $\nu_2$  are the complex positions of the mixed states (cf. explanations after Eq. (5)). The value of  $\text{Re}(\nu_1)$  should be compared to  $m_\rho^*$ ,  $\text{Re}(\nu_2)$  to  $m_\omega^*$ ,  $2\text{Im}(\nu_1)$  to  $\Gamma_\rho^*$  and  $2\text{Im}(\nu_2)$  to  $\Gamma_\omega^*$ . The mixing angles are defined in Eq. (6)

The first three cases assume that the  $\rho$  and  $\omega$  mesons have zero width, hence are of academic rather than practical interest. We list them, however, since the assumption of no width has been made in a number of calculations, such as the QCD sum rule calculations [14–16], or in the Walecka-model [10,11,18]. Case 1 assumes equal vector meson masses in symmetric matter,  $m_\rho^* = m_\omega^* = 500\text{MeV}$ . In this case in asymmetric medium we have ideal mixing, with  $\theta_1 = \theta_2 = 45^\circ$ , which results in splitting of masses by 66MeV. If  $m_\rho^*$  and  $m_\omega^*$  are split by 100MeV (case 2), then the mixing angles are equal to  $19^\circ$  and  $15^\circ$ , and additional splitting due to mixing is equal to 20MeV, a 20% effect compared to  $m_\rho^* - m_\omega^*$ . The increase of  $m_\rho^* - m_\omega^*$  to 200 MeV and simultaneous reduction of the wave-function renormalization (case 3) causes the reduction of the mixing angles to  $6^\circ$  and  $4^\circ$ . Note that such angles are still an order of magnitude larger than the mixing angle resulting from the electro-magnetic mixing. The remaining case have finite width of vector mesons. Cases 4-6 have  $m_\rho^* = m_\omega^*$ , large  $\Gamma_\rho^*$  and narrow  $\Gamma_\omega^*$ . We note that  $2\text{Im}(\nu_2)$  is significantly increased compared to  $\Gamma_\omega^*$  in cases 4 and 6, where  $\sqrt{Z_\rho^* Z_\omega^*} = 0.7$ . The mixing angles have large imaginary parts. Case 7 has  $m_\rho^* = m_\omega^*$  and  $\Gamma_\rho^* = \Gamma_\omega^* = 200\text{MeV}$ . In this case the mixing is ideal, with the mixing angle at  $45^\circ$ . Resonance positions and widths are shifted significantly. Cases 8-9 have  $m_\rho^* - m_\omega^* = 100\text{MeV}$ , wide  $\rho$  and narrow (case 8) or wide (case 9)  $\omega$ . Case 10 has  $m_\rho^* - m_\omega^* = 200\text{MeV}$ . Cases 11-12 take  $\rho_B = 3\rho_0$ , and, correspondingly, lower  $M^*$ , wider mesons, and smaller  $\sqrt{Z_\rho^* Z_\omega^*}$ . In cases 8-12 the mixing angles are in the range  $10 - 20^\circ$ . Cases 13-14 are for parameter set II, and should be directly compared to cases 8-9. We can see that the choice of parameters has very little influence on the mixing effect. To summarize, the mixing effects are sizeable for all sensible cases, with mixing angles of the order of  $10^\circ$ , or larger.

In order to be relevant for the physics of heavy-ion collisions, the above analysis has to be extended to finite temperatures. The most important effect of finite temperature

is the production of pions. We model these effects by assuming that we have ideal gas of protons, neutrons and pions in thermal equilibrium. The equilibrium with respect to the reactions  $p \leftrightarrow n + \pi^+$  and  $n \leftrightarrow p + \pi^-$  leads to the following relations among the chemical potentials for various components of the system:  $\mu_p = \mu_n + \mu_{\pi^+}$ ,  $\mu_n = \mu_p + \mu_{\pi^-}$ . The densities of particles are therefore given by

$$\rho_{p,n}(T) = 2 \int \frac{d^3k}{(2\pi)^3} \frac{1}{e^{\frac{\sqrt{M^{*2}+k^2}-\mu_{p,n}}}{T}} + 1}, \quad \rho_{\pi^\pm}(T) = \int \frac{d^3k}{(2\pi)^3} \frac{1}{e^{\frac{\sqrt{m_\pi^2+k^2} \mp (\mu_p - \mu_n)}{T}} - 1}. \quad (7)$$

There are two constraints in the system: the value of the baryon density and the electric charge density, which gets the contribution from protons and charged pions. Hence

$$\rho_p(T) + \rho_n(T) = \rho_B, \quad \rho_p(T) + \rho_{\pi^+}(T) - \rho_{\pi^-}(T) = \rho_p(T=0) \equiv \frac{1-x}{2} \rho_B, \quad (8)$$

where we have used the definition of  $x$  in the last equality. We solve Eq. (8) numerically for  $\mu_p$  and  $\mu_n$  at fixed  $\rho_B$  and  $x$ . Equipped with the chemical potentials we can now calculate  $\Pi_{\rho\omega}(\nu)$  at finite  $T$ . This is done by applying formula (4) with the replacement [32,33]

$$\theta(k_{p,n} - |\mathbf{k}|) \rightarrow (e^{\frac{\sqrt{M^{*2}+k^2}-\mu_{p,n}}}{T}} + 1)^{-1}. \quad (9)$$

The temperature effects can be described as follows. As we increase  $T$ , we produce pions, with the excess of  $\pi^-$  over  $\pi^+$ . The effect starts to be significant around  $T \sim m_\pi \sim 140\text{MeV}$ . The charge conservation constraint causes the reduction of the excess of neutrons over protons. As a result, the mixing element  $\Pi_{\rho\omega}(\nu)$  is reduced. Quantitatively, there is practically no effect for  $T$  up to 50MeV. At  $T \sim 140\text{MeV}$   $\Pi_{\rho\omega}(\nu)$  is reduced by about a factor of 2. This occurs for a variety of values of  $\nu$ ,  $M^*$  and  $\rho_B$ . Our analysis shows that the mixing effect will continue to be important at moderate temperatures. At higher temperatures, close to the chiral transition,  $\Pi_{\rho\omega}(\nu)$  is strongly suppressed, but our approach is no longer valid in that domain. Note that at higher  $T$  also the values of  $m_v^*$ ,  $\Gamma_v^*$ , and  $Z_v^*$  are strongly modified.

Clearly, other processes than that of Fig. 1 can also contribute to in-medium  $\rho$ - $\omega$  mixing, *e.g.* processes involving pions. It is unlikely, however, that such processes cancel the mechanism analyzed here. Thus, we expect that our results of large  $\rho$ - $\omega$  mixing will show up, among other possible medium-induced effects, in future high-accuracy relativistic heavy-ion experiments planned at GSI and CERN.

## References

- [1] For recent developments see *Quark Matter 96*, proc. 12th Int. Conf. on Ultra-Relativistic Nucleus-Nucleus Collisions, Heidelberg, Germany, 1996, Nucl. Phys. **A610**, and references therein
- [2] *Hadrons in Nuclear Matter*, edited by H. Feldmaier and W. Nörenberg (GSI, Darmstadt, 1995), proc. Int. Workshop XXIII on Gross Properties of Nuclei and Nuclear Excitations, Hirschegg, Austria, 1995
- [3] CERES Collab., G. Agakichiev *et al.*, Phys. Rev. Lett. **75** (1995)
- [4] HELIOS/3 Collab., M. Masera *et al.*, Nucl. Phys. **A590** (1995) 3c
- [5] G. Q. Li, C. M. Ko, and G. E. Brown, Nucl. Phys. **A606** (1996) 568
- [6] W. Cassing, W. Ehehalt, and C. M. Ko, Phys. Lett. **B363** (1995) 35
- [7] S. A. Chin, Ann. Phys. (NY) **108** (1977) 301
- [8] A. K. Dutt-Mazumder, B. Dutta-Roy, and A. Kundu, Phys. Lett. **B399** (1997) 196
- [9] B. D. Serot and J. D. Walecka, Advances in Nuclear Physics **16** (1986)
- [10] H. C. Jean, J. Piekarewicz, and A. G. Williams, Phys. Rev. **C49** (1994) 1981
- [11] H. Shiomi and T. Hatsuda, Phys. Lett. **B334** (1994) 281
- [12] G. E. Brown and M. Rho, Phys. Rev. Lett. **66** (1991) 2720
- [13] S. H. Lee, talk given at 13th International Conference on Ultrarelativistic Nucleus-Nucleus Collisions (*Quark Matter 97*), Tsukuba, Japan, 1-5 Dec 1997, SNUTP-98-009, hep-ph/9801338 (unpublished)
- [14] T. Hatsuda and S. H. Lee, Phys. Rev. **C46** (1993) R34
- [15] T. Hatsuda, S. H. Lee, and H. Shiomi, Phys. Rev. **C52** (1995) 3364
- [16] X. Jin and D. Leinweber, Phys. Rev. **C52** (1995) 3344
- [17] S. Leupold, W. Peters, and U. Mosel, Nucl. Phys. **A628** (1998) 311
- [18] T. Hatsuda, H. Shiomi, and H. Kuwabara, Prog. Theor. Phys. **95** (1996) 1009
- [19] G. Wolf, B. Friman, and M. Soyeur, GSI-preprint-97-37, nucl-th/9707055 (unpublished)
- [20] B. Friman and M. Soyeur, Nucl. Phys. **A600** (1996) 477
- [21] B. Friman and H. J. Pirner, Nucl. Phys. **A617** (1997) 496
- [22] B. Friman, talk given at APCTP Workshop on Astro-Hadron Physics: Properties of Hadrons in Matter, Seoul, Korea, 25-31 Oct 1997; GSI-preprint-98-7, nucl-th/9801053 (unpublished)
- [23] R. Rapp, G. Chanfray, and J. Wambach, Nucl. Phys. **A617** (1997) 472
- [24] F. Klingl, N. Kaiser, and W. Weise, Nucl. Phys. **A624** (1997) 527
- [25] F. Klingl and W. Weise, talk given at 36th Internationale Universitätswochen für Kernphysik und Teilchenphysik, Schladming, Austria, 1-8 March 1997; hep-ph/9802211 (unpublished)

- [26] K. Saito and A. W. Thomas, *Phys. Rev.* **C51** (1995) 2757
- [27] K. Saito, K. Tsushima, A. W. Thomas, and A. G. Williams, nucl-th/9804015 (unpublished)
- [28] J. J. Sakurai, *Currents and Mesons* (Univ. of Chicago Press, Chicago, 1969)
- [29] R. Machleidt, in *Advances in Nuclear Physics*, edited by J. W. Negele and E. Vogt (Plenum, New York, 1989), Vol. 19
- [30] W. Lenz, *Z. Phys.* **56** (1929) 778
- [31] C. D. Dover, J. Hüfner, and R. H. Lemmer, *Ann. Phys.* **66** (1971) 248
- [32] J. I. Kapusta, *Finite-Temperature Field Theory* (Cambridge University Press, Cambridge, 1989)
- [33] P. Rehberg and S. P. Klevansky, *Ann. Phys. (NY)* **252** (1996) 422



Table 1  
 $\rho$ - $\omega$  mixing in asymmetric matter. See text for details.

Input:	1	2	3	4	5	6	7	8	9	10	11	12	13	14
$\rho_B/\rho_0$	2	2	2	2	2	2	2	2	2	2	3	3	2	2
$M^*/M$	0.5	0.5	0.5	0.5	0.5	0.5	0.5	0.5	0.5	0.5	0.4	0.4	0.5	0.5
$m_\rho^*$ (MeV)	500	550	650	500	500	500	500	550	550	650	550	550	550	550
$m_\omega^*$ (MeV)	500	450	450	500	500	500	500	450	450	450	450	450	450	450
$\Gamma_\rho^*$ (MeV)	0	0	0	200	200	300	200	300	300	300	400	400	300	300
$\Gamma_\omega^*$ (MeV)	0	0	0	50	50	50	200	50	200	200	300	300	50	200
$\sqrt{Z_\rho^* Z_\omega^*}$	0.7	0.7	0.35	0.7	0.35	0.7	0.7	0.7	0.7	0.7	0.5	0.3	0.7	0.7
Output, $x = x_{pb}$ :	Set I												Set II	
$\text{Re}(\nu_1)$ (MeV)	535	562	652	509	502	505	532	557	559	656	559	553	555	557
$\text{Re}(\nu_2)$ (MeV)	469	442	449	494	499	497	470	445	443	446	442	447	446	444
$2\text{Im}(\nu_1)$ (MeV)	0	0	0	170	193	286	218	298	306	309	414	405	297	302
$2\text{Im}(\nu_2)$ (MeV)	0	0	0	83	57	67	186	56	198	198	294	298	55	200
$\text{Re}(\theta_1)$ (deg)	45	19	6	12	3	5	45	11	17	11	18	11	9	14
$\text{Re}(\theta_2)$ (deg)	45	15	4	11	2	4	45	8	13	7	14	9	7	12
$\text{Im}(\theta_1)$ (deg)	0	0	0	-31	-13	-15	0	-7	-1	2	1	1	-6	-2
$\text{Im}(\theta_2)$ (deg)	0	0	0	-32	-13	-16	0	-6	-2	0	0	0	-6	-2